



SEISMIC STRUCTURE SOIL-STRUCTURE INTERACTION (SSSI) EFFECTS FOR DENSE URBAN AREAS

Dan M. GHIOCEL¹, Ovidiu BOGDAN² and Dan CRETU³

ABSTRACT

The paper presents selected results of an international project of the new research center in earthquake engineering entitled “*Dan Ghiocel International Research Center*” at Technical University of Civil Engineering, Bucharest, Romania. The paper investigates the seismic structure-soil-structure interaction effects (SSSI) in densely built urban areas for a 15 floor Multistory Building (MB), a Church Building (CB) and a Subway Station (SS) in the Bucharest city. A description of the SSI effects for each of the three standalone buildings is provided in a companion paper (Bogdan, Ghiocel and Cretu, 2014). Seismic input was defined by a set of three-directional spectrum compatible acceleration histories generated based on the Romanian seismic design spectrum for the Bucharest city area. The seismic SSI and SSSI analyses were performed using the state-of-the-art ACS SASSI software. Three SSSI layout scenarios were considered. The SSSI analyses were performed for both coherent (synchronous) and incoherent (non-synchronous) seismic inputs. Based on the investigated case studies, the paper concludes that SSSI effects can be quite significant, especially when the seismic motion spatial variation in horizontal directions is also included.

SEISMIC SSI ANALYSIS METHODOLOGY AND INPUTS

The seismic SSI and SSSI analyses were performed using the ACS SASSI software (Ghiocel, 2013). The ACS SASSI software uses the flexible volume substructuring (FVS) in complex frequency to perform accurate and efficient SSI analyses for embedded or buried structures under coherent and incoherent seismic waves, or other external dynamic excitations from explosions, traffic, turbine vibrations, or other vibration sources. Using FVS in the complex frequency domain the SSI system damping matrix was included as a non-proportional matrix and the structural and soil material damping can be modelled as a hysteretic type damping that is independent of frequency as evidenced by various experimental lab tests. This is not possible in time-domain by using frequency-dependent damping such as the Rayleigh damping.

Using the FVS approach there is no need to include a large zone of the soil deposit in the FE model. This saves huge computational effort. In complex frequency, the lateral and bottom frequency-dependent transmitting boundaries of the FE model can be placed directly at the interface between the foundation and soil media with no impact on the SSI solution accuracy. Such a type of substructuring is not possible in time-domain, since the frequency-dependent nature of the soil dynamic behaviour cannot be modeled by placing transmitting boundaries directly at the foundation-soil interface. The FVS exploits at maximum the numerical efficiency of the consistent transmitting boundaries since the

¹ Chief of Engineering, Ghiocel Predictive Technologies, Inc., Rochester, New York, and Adjunct Professor, Case Western Reserve University, Cleveland, Ohio, USA, dan.ghiocel@ghiocel-tech.com

² Lecturer, Technical University of Civil Engineering, Bucharest, Romania, obogdan@utcb.ro

³ Professor, Technical University of Civil Engineering, Bucharest, Romania, cretud@utcb.ro

seismic load vector is computed as a product of the free-field soil motions and the free-field soil impedances for the excavated soil dofs. Thus, FVS makes the soil impedance and input motion calculations trivial and extremely fast.

The FVS approach basically replaces the *external source* dynamic problem that assumes a large-size SSI FE model, including the structure plus a large zone of soil deposit, excited by a seismic motion defined at the far-distant bottom and lateral soil foundation boundaries with a reduced-size problem that is an *internal source* dynamic problem that assumes a reduced FE model, including only the structure and the excavated soil (internal to the basement) instead of including the entire surrounding soil deposit (that needs to be extended for a large zone to simulate the soil boundless) excited by a seismic excitation defined at the excavated soil dofs.

Both coherent and incoherent motions were considered. The ACS SASSI software includes a number plane-wave incoherency models for capturing the seismic motion spatial variation in horizontal plane. In contrast to the simplified, traditional representation of the seismic wave field by coherent motions, the incoherent motions are a much more accurate idealization of the seismic random wave fields including the three-dimensional seismic wave propagation aspects. Incoherent motions are simulated based on the stochastic models developed based on the dense array real record databases. From a theoretical point of view, the soil motion spatial variation is idealized by a space-time Gaussian stochastic process (or field). The soil motion spatial variability is completely defined by the stochastic process coherency spectrum or coherence function that corresponds to the intense part of the seismic motion (defined between 5% and 75% or the Arias intensity). The incoherent motion was idealized based the Abrahamson plane-wave coherency model applicable to soil sites (Abrahamson, 2007) including a wave passage effect defined for an apparent horizontal wave velocity of 1,300m/s along a direction that makes 45 degree angle with the principal axes of the MB structure.

The seismic input at the ground surface was defined by a set of three-component spectrum compatible acceleration histories generated based on the Romanian P100-206 seismic design code spectrum for the Bucharest city area (Bogdan, Ghiocel and Cretu, 2013). Figure 1 shows the generated spectrum compatible acceleration history input for the X direction and the associated 5% damping response spectrum. Similar acceleration history inputs were generated for the Y and Z directions. The ZPGA was 0.20g for X and Y (horizontal) components and 0.14g for Z (vertical) component.

The soil conditions consist of a deep soft soil deposit with a slowly varying shear wave velocity value from 260m/s at ground surface to 440m/s at a depth of 100m. Figure 2 shows the shear wave velocity soil profile.

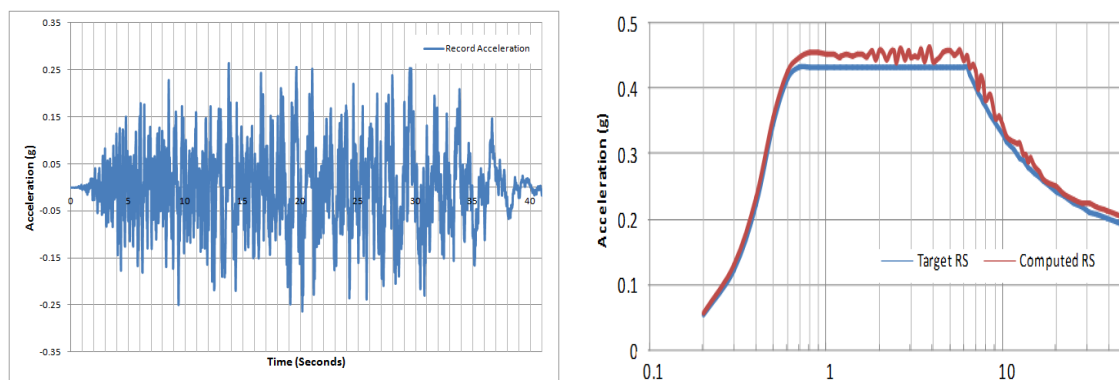


Figure 1 Acceleration History Input and Associated 5% Damping Response Spectra for X-Direction

Figure 3 shows the layouts of the SSSI models that were considered in the study: i) SSSI Model 2 consists of MB in the longitudinal direction being parallel to SS and CB in the longitudinal direction as shown in Figure 3 left plot, ii) SSSI Model 3 consists of MB in the longitudinal direction being perpendicular to SS in the longitudinal direction and being parallel to CB in longitudinal direction as shown in Figure 3 right plot. The SSSI Model 1 is identical with SSSI Model 3 except that CB is not included.

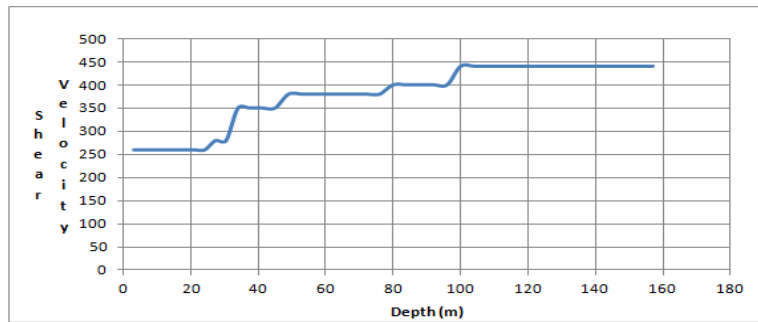


Figure 2 Vs Profile for Soil Deposit Layering at the Investigated Site in Bucharest

It should be noted that the MB SSI model has three levels of embedment, with a foundation level at the 10m depth, the CB SSI model has no embedment, and the SS SSI model is fully embedded, with a foundation level at 24m depth. The distance between the MB and SS buildings was varied from 1m to 5m.

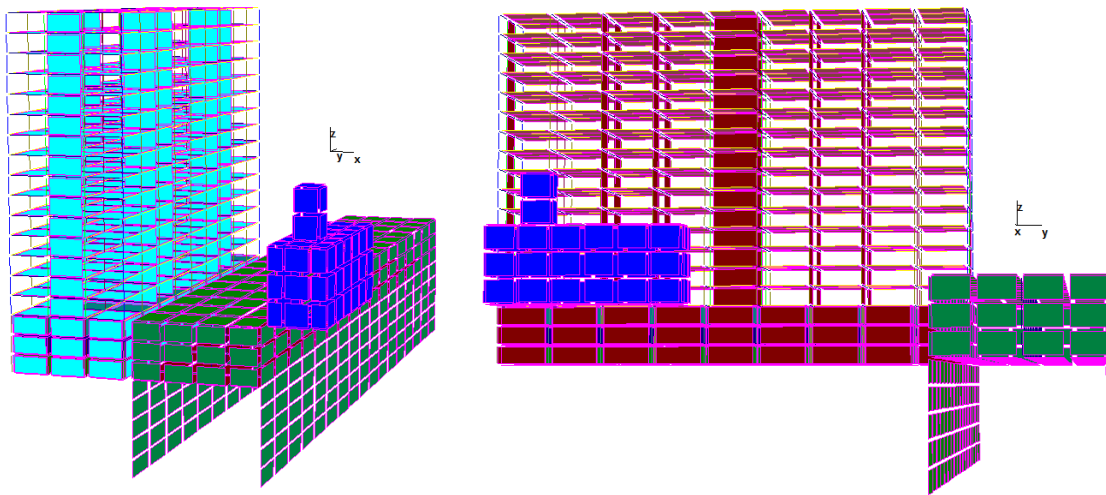


Figure 3 Seismic SSSI Analysis Models: SSSI Model 2 (left plot) and SSSI Model 3 (right plot)

The seismic SSSI analysis results and the standalone SSI analysis results were compared for each of the three buildings and the three SSSI layout scenarios. The SSI and SSSI analysis result comparisons were done in terms of i) the maximum acceleration (ZPA) profiles on the buildings, ii) the 5% damping acceleration response spectra (ARS) at different elevations in the three structures, and iii) the structural forces and bending moments computed in the MB corner columns and in the MB and SS external shearwalls at the closest locations between the MB and SS structures.

SEISMIC COHERENT MOTION ANALYSIS RESULTS

In this section the coherent standalone SSI results were compared with the coherent SSSI results obtained for the building layouts shown in Figure 3.

Figure 4 shows the comparison of the maximum acceleration or ZPA profiles on the MB structure computed in the horizontal and vertical directions for the closest column to SS. The computed variations were up to 20%.

Figure 5 shows the 5% damping horizontal ARS computed at the MB roof-level for the corner location the closest to SS. It should be noted that the SSSI effects amplify the MB response in the direction of the MB-SS alignment. The SSSI amplifications were up to 20%.

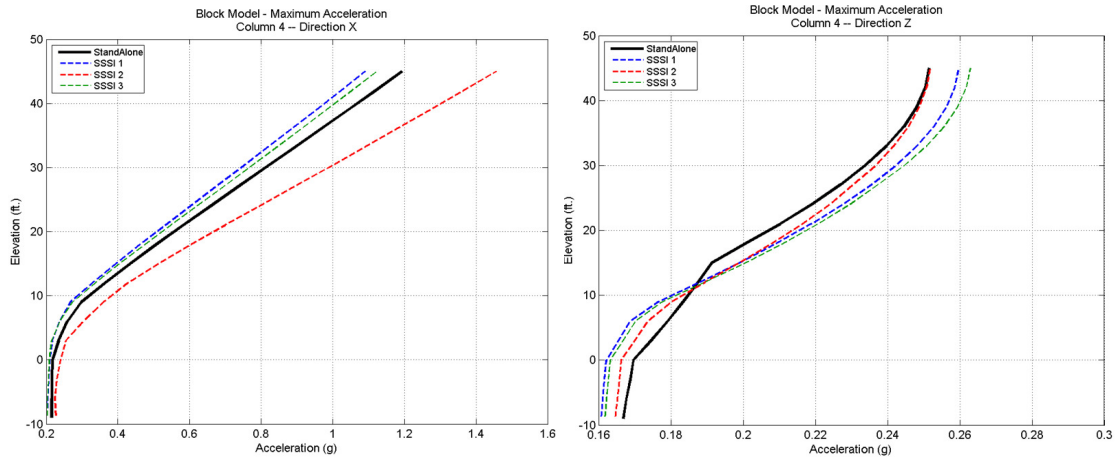


Figure 4 The Horizontal (left) and Vertical (right) ZPA Profiles on the MB Structure for Column 4 Line that is the Closest to SS

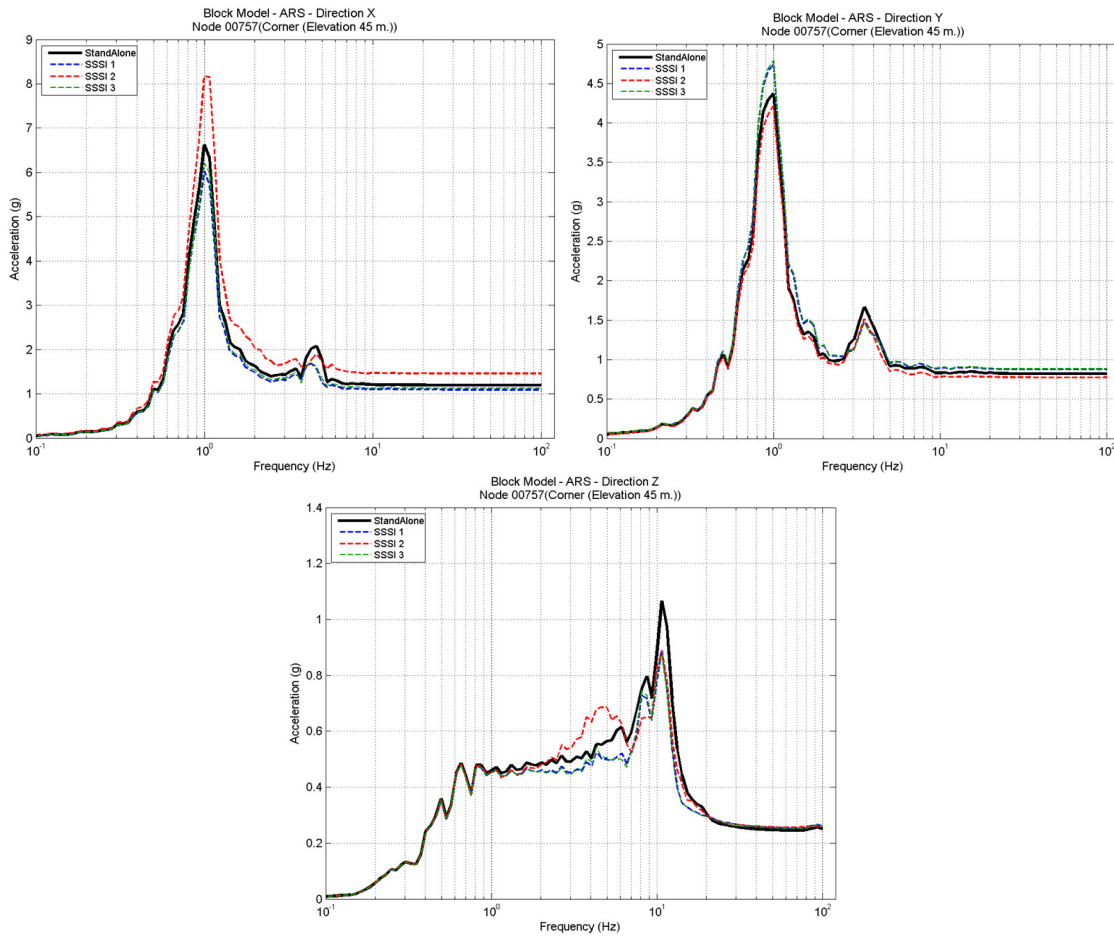


Figure 5 SSSI Effects on the MB Roof ARS (Elevation 45m) at the Corner Location Closest to SS, for X direction (left-upper), Y direction (right-upper) and Z direction (middle-lower)

Figure 6 shows the SSSI effects on the forces and bending moments in the MB corner column line closest to SS, Column 4. Figure 7 shows the SSSI effects on the in-plane shear and forces in the

MB shearwall closest to SS. It should be noted that SSSI effects could produce relatively modest amplifications in the structural forces of about 10%-15%.

Figure 8 shows the SSSI effects on the 5% damping ARS computed at the roof level of the smaller CB structure. In the transverse direction, the SSSI effects are significant for the SSSI Model 2 and negligible for SSSI Model3. In SSSI Model 2, the surface CB structure is placed very close, along the deeply embedded SS structure.

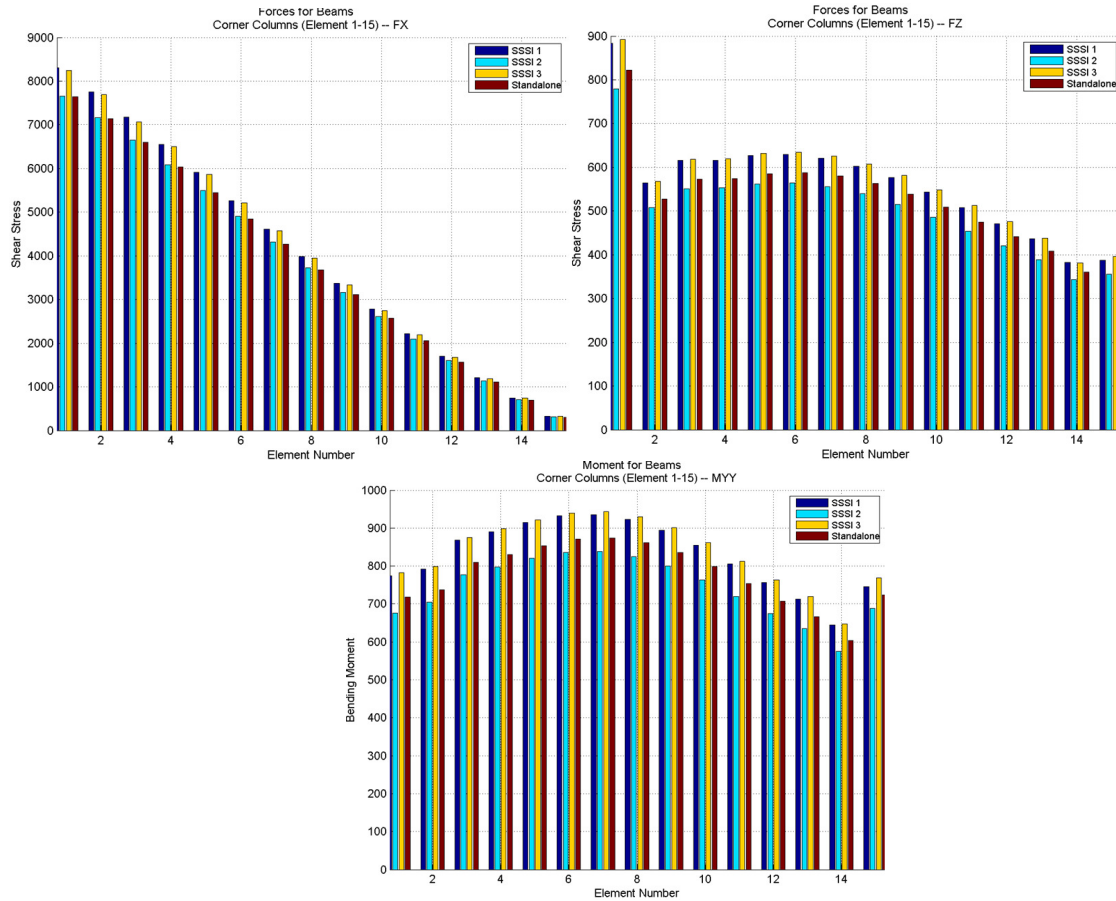


Figure 6 SSSI Effects on the Axial (left-upper), Shear Forces (right-upper) and Bending Moments (middle-lower) Per Unit Length in the MB Corner Column Closest to the SS Structure

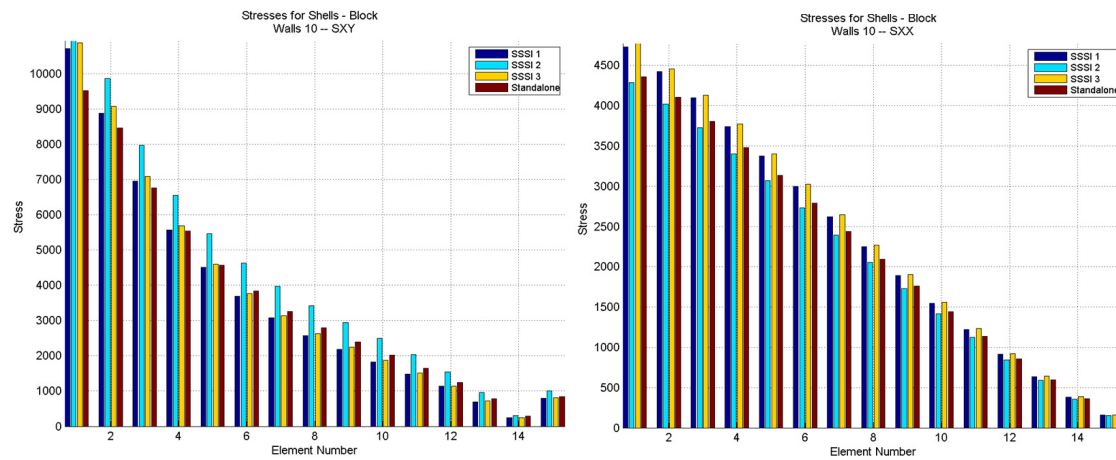


Figure 7 SSSI Effects on the In-Plane Shear and Normal Forces per Unit Length (kN/m) in the MB External Transverse Shearwall Closest to the SS Structure

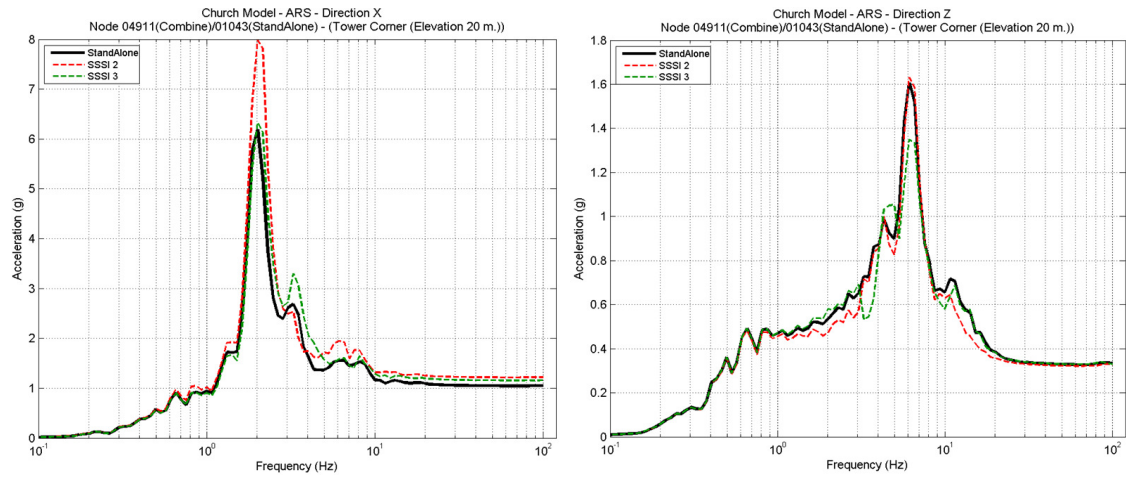


Figure 8 SSSI Effects on the Transverse ARS (left) and Vertical ARS (right) in the CB Structure at Roof Level (Elevation 20m)

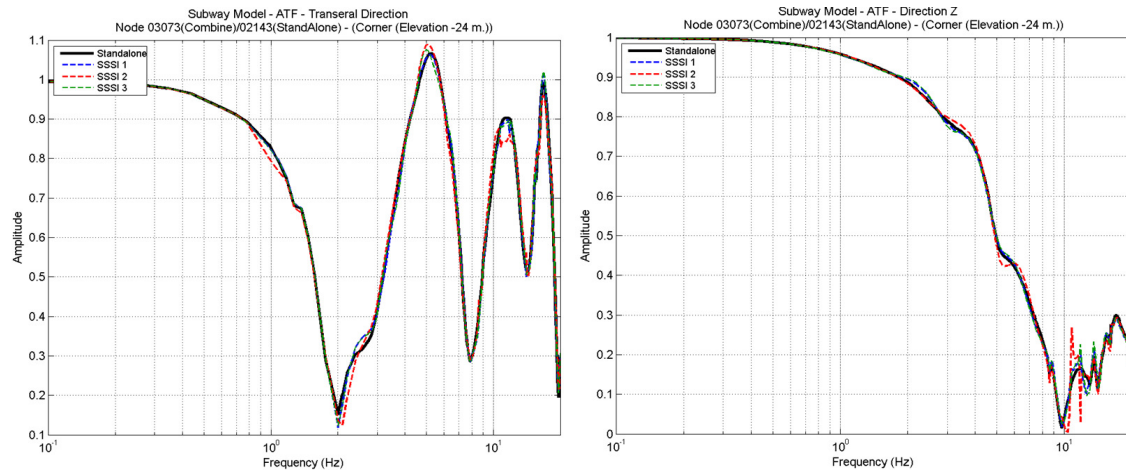


Figure 9 SSSI Effects on the Transverse ATF (left) and Vertical ATF (right) at the SS Foundation Level (Elevation -24m)

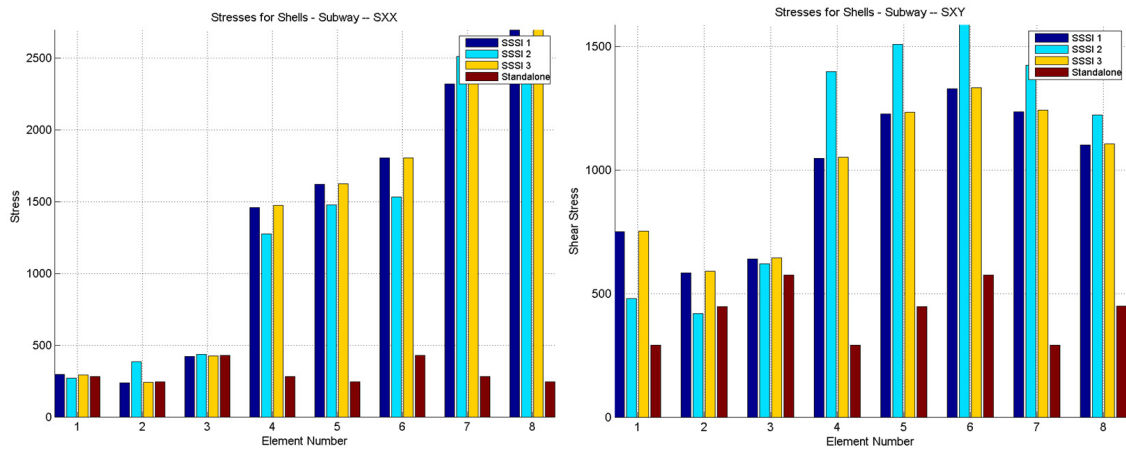


Figure 10 SSSI Effects on the In-Plane Shear and Normal Forces per Unit Length (kN/m) in the SS Lateral Shearwall that is Closest to the MB Structure

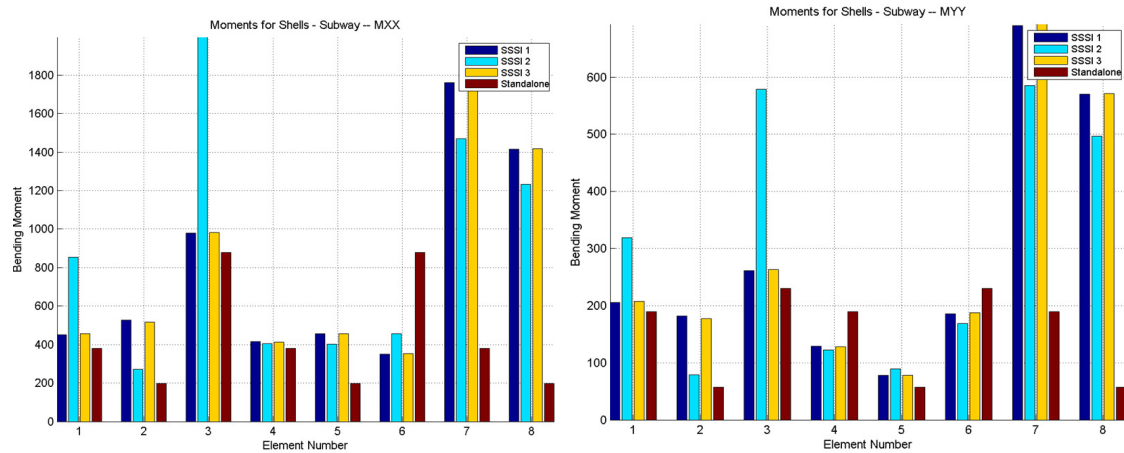


Figure 11 SSSI Effects on the Out-of-Plane Bending Moments MXX and MYX per Unit Length (kN-m/m) in the SS Lateral Shearwall that is Closest to the MB Structure

Figure 9 shows the acceleration transfer function (ATF) amplitude at the SS foundation level at the 24 m depth. The computed ATF at foundation level indicate that the SS acceleration motion is practically the same for the standalone SSI model and the SSSI models. It should be noted that the ATF responses of SS in Figure 9 describe only the inertial SSSI effects on CB, and not the kinematic SSSI effects due to soil differential motions that are expected to be dominant for a deeply embedded structure such as SS.

Figures 10 and 11 show the maximum in-plane forces and out-of-plane bending moments in a vertical slice of the SS shearwall that is the closest to the MB structure. The wall stresses increase up to 4-5 times due to the SSSI effects. The presence of the embedded MB structure in the vicinity of SS produces a large amplification of the soil seismic pressures on the SS embedded walls, a result of kinematic SSSI effects .

Sensitivity studies have indicated that SSSI effects are still very important even for larger distances up to 5m between MB and SS. No investigation was done at this time for a separation distance between MB and SS larger than 5m.

COMPARISONS OF COHERENT AND INCOHERENT SSSI ANALYSIS RESULTS

In this section the coherent SSSI results are compared with the incoherent SSSI results. The comparison is limited to the SSSI Model 3 building layout arrangement (Figure 3, right plot).

The incoherent motion was idealized based the Abrahamson plane-wave coherency model applicable to soil sites (Abrahamson, 2007) including also a wave passage effect with an apparent horizontal wave velocity of 1,300 m/s along the propagation direction that makes a 45 degree angle with the principal axes of the MB structure.

Figures 12, 13 and 14 show a comparison between the coherent SSSI coherent and incoherent SSSI horizontal and vertical ZPA profiles in the X, Y and Z directions for the MB corner column lines that are the closest (Column 4) and the farthest (Column 2) to the SS structure. The incoherent SSSI responses were obtained using the ACS SASSI stochastic approach with 10 random field simulations.

It should be noted that for some stochastic simulations of the incoherent seismic wave field, the incoherent SSSI results were significantly larger than the coherent SSSI results. For the transverse direction of the MB structure, as shown in Figure 12, the maximum accelerations could be up to 30-40% larger for some incoherent SSSI samples than the coherent SSSI. Also, there is a larger variation of the incoherent response for Column 2 line that is far from SS, than for Column 4 line, that is close to SS. In the longitudinal direction of MB, as shown in Figure 13, for most of the incoherent SSSI random samples the maximum accelerations are slightly lower than for the coherent SSSI.

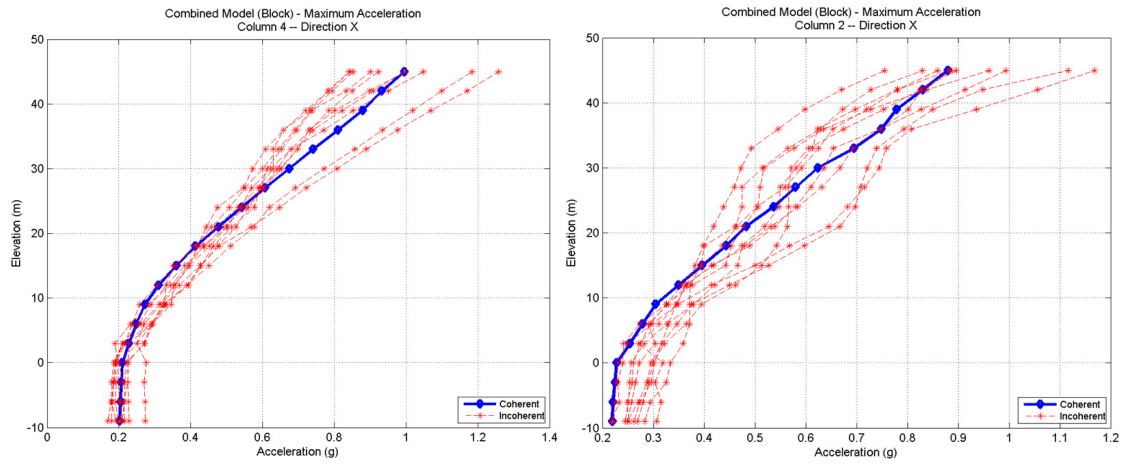


Figure 12 ZPA Profiles in Transverse Direction for the MB Column 4 (left) and Column 2 (right)

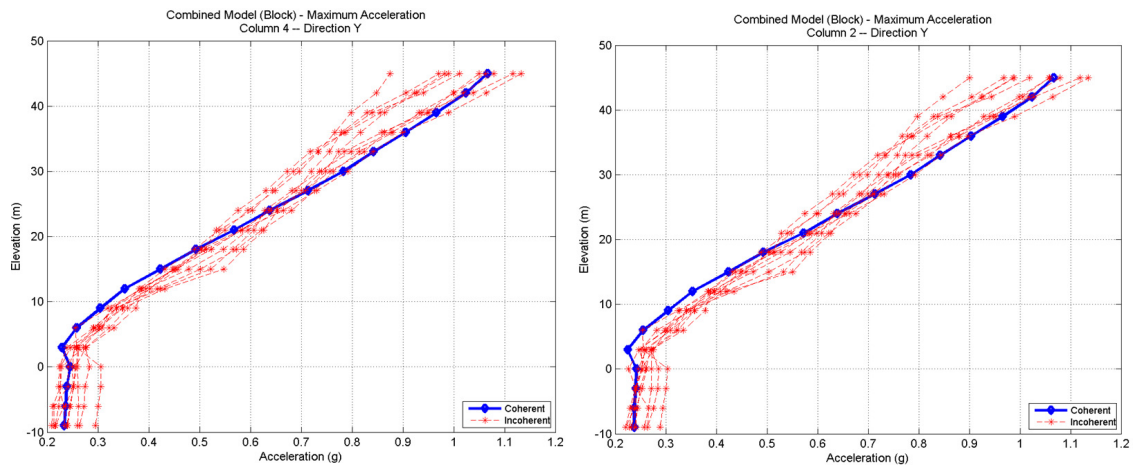


Figure 13 ZPA Profiles in Longitudinal Direction for the MB Column 4 (left) and Column 2 (right)

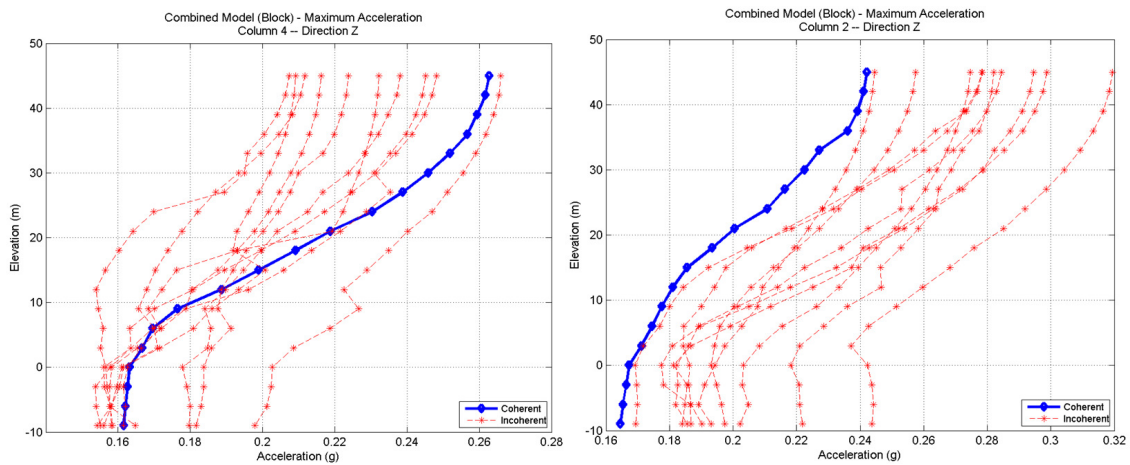


Figure 14 ZPA Profiles in Vertical Direction for the MB Column 4 (left) and Column 2 (right)

For the vertical maximum accelerations shown in Figure 14, most of the incoherent SSSI response samples are lower than coherent SSSI response for Column 4 and larger for Column 2. The Column 2 vertical ZPA profile is in average about 20% larger than the Column 4 vertical ZPA profile.

This is a typical behaviour for a shallow foundation structure as MB sitting nearby a deeply embedded structure as SS. It is due to the scattered Rayleigh wave reflected from the embedded walls that amplifies the vertical motion amplification at the MB foundation level at the far end

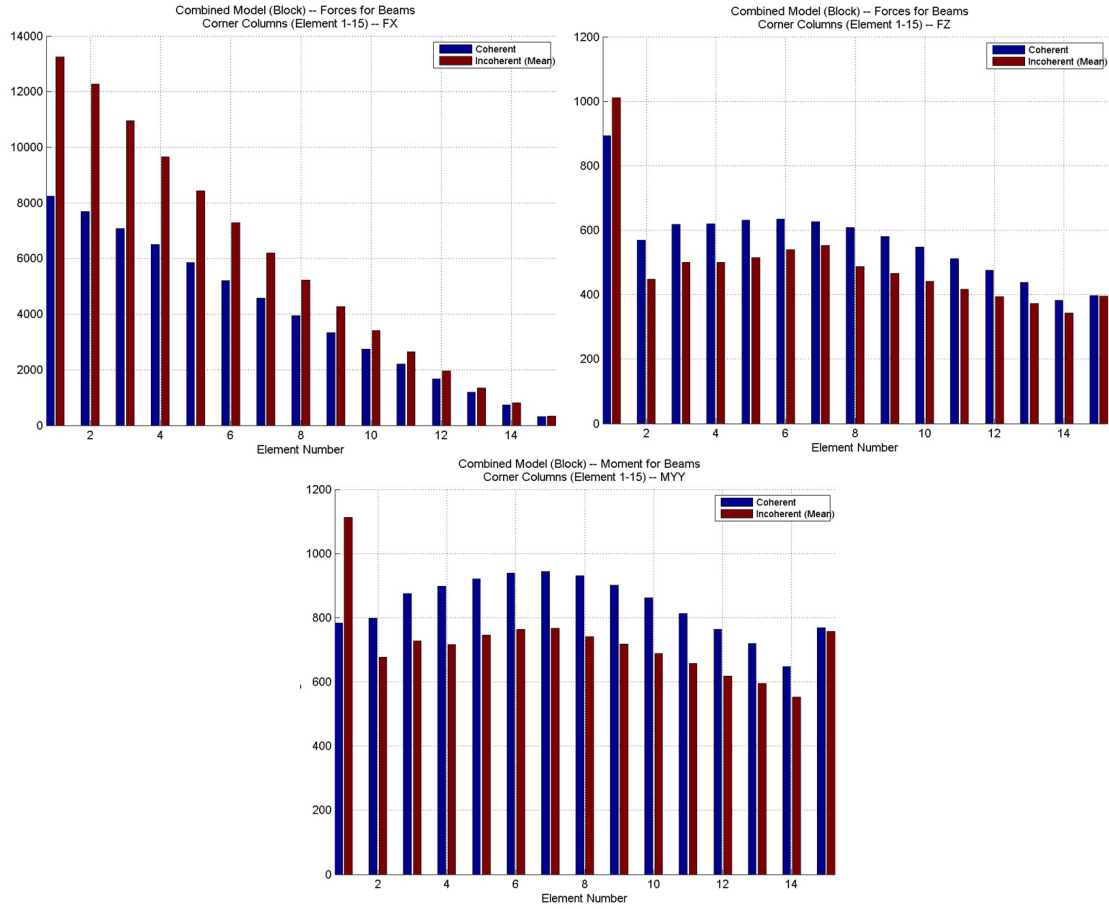


Figure 15 The Axial Force (left-upper), Shear Force (right-upper) and Bending Moment (middle-lower) (Per Unit Length) Diagram in the MB Column 2 Line

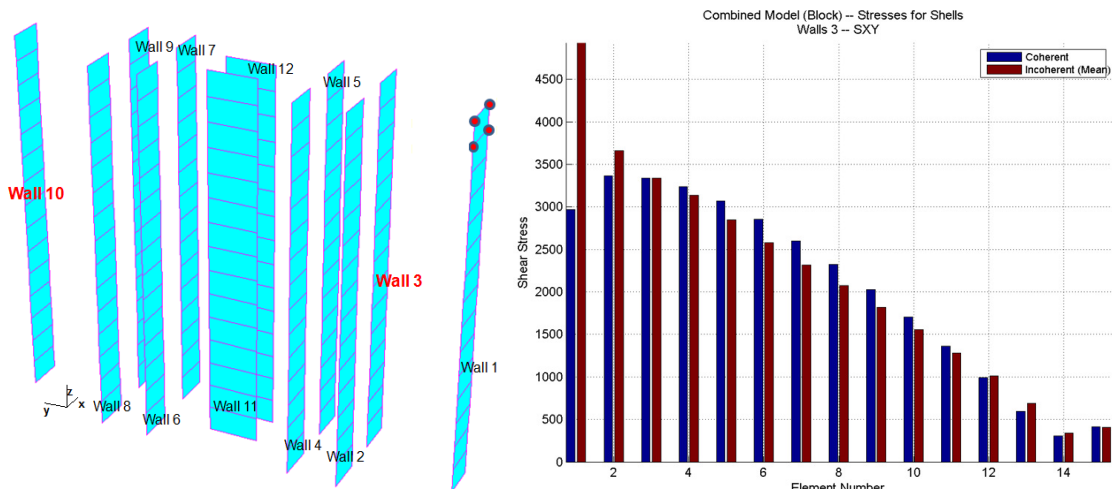


Figure 16 The In-Plane Shear (right) per Unit Length (kN/m) in the MB Shearwall (Wall 3 in left plot) that is Close to the SS Foundation Walls (SS is placed on right side of the plot - see also Figure 3)

Figure 15 shows the axial, shear forces and bending moments in the MB corner Column 2 line. It should be noted that the *mean* incoherent SSSI axial force response is much larger, above 50% higher than the coherent SSSI axial force response.

For the computed shear force and bending moments in the MB Column 2 line, the *mean* incoherent SSSI responses are slightly lower, except for the first floor for which the *mean* incoherent responses are larger by 15-30% than the coherent SSSI responses.

Figure 16 shows the comparisons of the shear forces computed in one of the MB internal shearwalls (Wall 3 in left plot) that are close to the SS structure. The *mean* incoherent SSSI shear force and the coherent SSSI shear force in the shearwall are about the same, except at the first floor for which the *mean* incoherent SSSI response is above 50% larger than the coherent SSSI response.

It should be noted, although it is not shown herein, that incoherent SSSI response simulations might have responses significantly larger than the coherent SSSI response, up to twice of the coherent amplitudes. These results indicate the important role of the motion spatial incoherency (non-synchronous character) on the SSSI responses. These incoherent SSSI response amplifications produced by the random SSSI wave scattering effects that could be much larger for the incoherent wave motions than for the coherent wave motions.

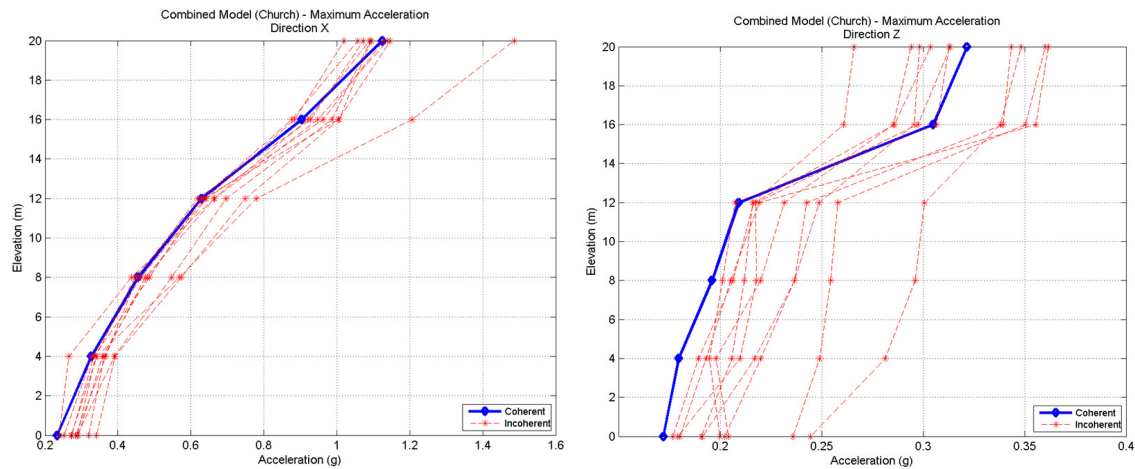


Figure 17 SSSI Effects on Horizontal ZPA (left) and Vertical ZPA Profiles (right) for the CB Structure

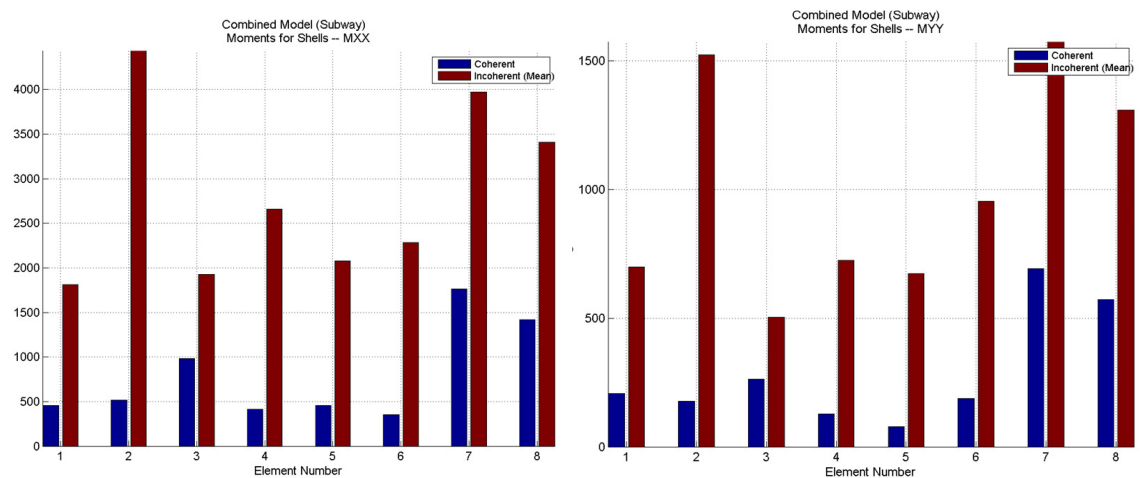


Figure 18 SSSI Effects on Out-of-Plane Bending Moments MXX (left) and MYY (right) Per Unit Length (kN-m/m) in the SS Shearwall that is the Closest to the MB Structure

Figure 17 shows a comparison of the maximum acceleration profiles for the CB structure. The motion incoherency effect on the CB structure is to amplify the SSSI response, especially in the vertical

direction due to the randomly scattered Rayleigh wave components moving from SS and MB toward the CB structure.

Figure 18 shows the effect of motion incoherency on the SSSI responses expressed in terms of the forces and moments in the SS embedded shearwalls. The plotted results are computed for a vertical wall slice that is the closest to the MB structure. The motion incoherency impacts severely on the SS structure walls. The presence of the MB structure produces randomly scattered waves that amplify considerably the dynamic soil pressures on the SS embedded walls.

It should be noted that these large amplifications by 200-300% of the SS wall bending moments due to the motion incoherency SSSI effects are in addition to the amplifications by 200-300% of the SS wall bending moments due to the coherent SSSI effects shown in Figure 11. Thus, the overall incoherent SSSI elastic response against the standalone SSI elastic response in terms of the SS embedded wall bending could be up to 10 times larger. If the SS walls are not largely oversized (typically by using the free-field soil strain applied to the embedded structure), then, the incoherent SSSI phenomena will produce significant damages in this embedded structure. It would be of critical importance that the SS walls have large ductility capabilities to resist to much larger structural loads produced by the incoherent SSSI effects.

CONCLUDING REMARKS

The paper opens a new perspective for seismic structural design in dense urban areas. The traditional seismic design approach that is based solely on the application of external seismic forces on the superstructure ignores the seismic random wave scattering and SSSI coupling effects for neighbour buildings that occur during earthquakes in dense urban areas. These effects are combined effects of the SSSI coupling and the motion spatial variations due to incoherency.

The paper concludes that for the investigated case studies, the incoherent SSSI effects are significant, non-negligible for the MB and CB structures, and extremely large for the deeply embedded SS structure. The coherent SSSI effects are more modest, but the coherent SSSI analysis is based on a less realistic assumption for modelling the seismic wave field that neglects the soil motion variability in horizontal directions, which is a known fact, proven by many earthquake motions recorded in dense arrays at various locations around the globe.

The paper *urges* the earthquake engineering communities to pay attention to the combined SSSI and motion incoherency effects in dense urban areas since these significant dynamic coupling effects are currently ignored in seismic design.

REFERENCES

- Abrahamson, N. (2007). "Effects of Seismic Motion Incoherency Effects" Electric Power Research Institute, Palo Alto, CA and US Department of Energy, Germantown, MD, Report No. TR-1015110, December 20
- Bogdan, O., Ghiocel, D.M. and Cretu, D. (2014). "Seismic Soil-Structure Interaction (SSI) for Different Types of Buildings in Dense Urban Areas", *the 2nd European Conference on Earthquake Engineering and Seismology*, 2ECEEE, Istanbul, August 25-29.
- Ghiocel, D.M. (2013). "ACS SASSI Version 2.3.0 - An Advanced Computational Software for 3D Seismic Analyses Including Soil-Structure Interaction", *Ghiocel Predictive Technologies, Inc.* (www.ghiocel-tech.com/enggTools/ACS%20SASSI_V230_Brief_Description_Jan_2014.pdf)
- Ghiocel, D.M., Li, D. Brown, H., Zhang, J. (2010). "EPRI AP1000 NI Model Studies on Seismic Structure-Soil-Structure Interaction (SSSI) Effects" *OECD NEA Seismic SSI Workshop*, Ottawa, October 6-10
- Ghiocel, D.M., Todorovski, L., Fuyama, H. and Mitsuzawa, D., (2011) "Seismic Incoherent Soil-Structure Analysis of A Reactor Building Complex on A Rock Site", *SMIRT 21 Proceedings*, Division V, Paper 825, New Delhi, India, November 6-11
- Yue, D., Ghiocel, D.M., Fuyama, H., Ogata, T. and Stark, G. (2013) "Structure-Soil-Structure Interaction Effects for Two Heavy NPP Buildings With Large-Size Embedded Foundations", *SMIRT22 Proceedings*, Division V, San Francisco, California, August 18-23